

# Shape Evolution of Silver Nanoplates through Heating and Photoinduction

Bin Tang,<sup>†</sup> Shuping Xu,<sup>‡</sup> Xueliang Hou,<sup>†</sup> Jingliang Li,<sup>†</sup> Lu Sun,<sup>\*,†,§</sup> Weiqing Xu,<sup>‡</sup> and Xungai Wang<sup>\*,†,§</sup>

<sup>†</sup>Institute for Frontier Materials, Deakin University, Geelong, Victoria 3216, Australia

<sup>‡</sup>State Key Laboratory of Supramolecular Structure and Materials, Jilin University, Changchun 130012, P. R. China

<sup>§</sup>School of Textile Science & Engineering, Wuhan Textile University, Wuhan 430073, China

## S Supporting Information

**ABSTRACT:** Shape conversions of silver nanoplates were realized by heating and subsequent light irradiation. The initial silver nanoprisms were transformed into silver nanodisks gradually in the process of heating, which was possibly achieved through dissolving and reabsorption of silver atoms on the surface of silver nanoplates. Subsequently, under light irradiation, the heating induced silver nanodisks were reversed to silver nanoprisms in the same solution. The dissolved oxygen was found to play a pivotal role in the shape conversion from nanoprism to nanodisk. In addition to heating, deionized water could induce the shape conversion of silver nanoplates when it was added to precipitate of the initial silver nanoprisms after centrifugation. Citrate in solution is essential to the photoinduced shape conversion process. Transmission electron microscopy (TEM) and extinction spectroscopy results demonstrated that localized surface plasmon resonance (LSPR) properties of silver nanoplates were effectively tuned through shape conversion.

**KEYWORDS:** silver nanoparticles, shape conversion, heating aging, light irradiation, nanodisks, nanoprisms, localized surface plasmon resonance



deionized water could induce the shape conversion of silver nanoplates when it was added to precipitate of the initial silver nanoprisms after centrifugation. Citrate in solution is essential to the photoinduced shape conversion process. Transmission electron microscopy (TEM) and extinction spectroscopy results demonstrated that localized surface plasmon resonance (LSPR) properties of silver nanoplates were effectively tuned through shape conversion.

## 1. INTRODUCTION

Shape-controlled synthesis of noble metal nanoparticles, in particular silver and gold nanostructures, has attracted increasing attention because of their great potential for applications in surface enhanced spectroscopy,<sup>1–3</sup> biological and chemical sensing,<sup>4,5</sup> and diagnosis and therapy of diseases.<sup>6,7</sup> Most of these applications are based on the unique optical properties of noble metal nanostructures, which are known as localized surface plasmon resonance (LSPR).<sup>8–11</sup> The LSPR of noble metal nanoparticles depends on their size, shape, composition and surroundings.<sup>12–16</sup> Among the noble metal nanostructures, the LSPR of silver nanoplates can be easily tuned by controlling the aspect ratios and shapes. Many strategies have been developed to synthesize silver nanoplates and tailor their morphologies, such as photoinduction,<sup>17,18</sup> thermal treatment,<sup>19–23</sup> ion etching,<sup>24–26</sup> sonochemical treatment,<sup>27–30</sup> ligand-assisted method<sup>28,31,32</sup> and surfactant-free synthesis route.<sup>33,34</sup> Photoinduction as an effective preparation route for silver nanoplates was first reported by Mirkin et al.<sup>17</sup> Subsequently, a number of approaches based on photoinduction have been used to synthesize the anisotropic silver nanoparticles with stereostructures, such as tetrahedron,<sup>35,36</sup> decahedron<sup>37–39</sup> and bipyramid.<sup>40</sup> In the photoinduced route for synthesis of silver nanoparticles, the final size and shape were found to strongly depend on excitation wavelength of light sources.<sup>18,41–45</sup> Besides the photoinduction method,

thermal treatment is also performed widely to produce silver nanoplates with different shapes. Sun et al. prepared triangular silver nanoplates with sharp corners in the presence of poly(vinylpyrrolidone) (PVP) and sodium citrate by refluxing aqueous dispersions of spherical silver colloids.<sup>19</sup>

In addition to direct synthesis of anisotropic silver nanoparticles, post conversion methods for controlling the shape of silver nanoparticles were also developed. Chen et al. synthesized silver nanodisks from triangular nanoplates in the presence of cetyltrimethylammonium bromide (CTAB), through an aging process at 40 °C.<sup>21</sup> Also, uniform discal silver nanoplates were synthesized from silver nanoprisms by heat aging in our previous report.<sup>30</sup> The size and LSPR of the nanoplates could be easily adjusted by controlling the heating time during aging process. Furthermore, triangular silver nanoplates were transformed into nanodisks through a UV irradiation method by Yin et al.<sup>46</sup> In their research, PVP was added into as-prepared samples to stabilize the silver nanoplates and the LSPR property of silver nanoplates was adjusted in the photoinduced reconstruction process. The hexagonal silver nanoplates were also prepared through transformation from triangular silver nanoplates by a photoinduction approach.<sup>47</sup>

**Received:** September 21, 2012

**Accepted:** January 8, 2013

**Published:** January 8, 2013

Additionally, shape conversion and reconstruction of silver nanoprisms were also achieved by us using a photoinduction technology, in which a series of shape conversions from nanoprism to nanodisk, and then back to nanoprism were realized by controlling the citrate concentrations in solution during the photoinduction process.<sup>48</sup> Additional stabilizers or structure directing agents were needed to achieve the shape conversion. For tuning the optical properties of silver nanoparticles, it is important to accomplish a series of shape conversions of silver nanoparticles without changing any components of the reaction system.

Herein, shape conversion and reconstruction of silver nanoplates were achieved by heating and subsequent irradiating under a sodium lamp in the same reaction system. LSPR properties of silver nanoplates were effectively adjusted over a certain range in the process of shape conversion. Mechanism of shape conversion for silver nanoplates is discussed. The effects of dissolved oxygen and citrate on shape conversion of silver nanoplates are investigated.

## 2. EXPERIMENTAL SECTION

**2.1. Materials.** AgNO<sub>3</sub> (>99%), trisodium citrate (≥99.0%), sodium borohydride (>98%), sodium L-tartrate dibasic dihydrate (≥99%), PVP ( $M_w = 40,000 \text{ g mol}^{-1}$ ) and hydrogen peroxide (30 wt %) were purchased from Sigma-Aldrich. All chemicals were of analytical grade, and used without further purification.

**2.2. Instruments.** Extinction spectra of silver nanoparticle solutions were recorded using a Varian Cary 3E UV/vis spectrophotometer. Transmission electron microscopy (TEM) images were obtained using a JEM-2100 with an acceleration voltage of 200 kV. Samples for TEM analysis were prepared by dripping a drop of silver nanoparticle solutions onto the carbon coated copper grids and drying them in the air at room temperature. A Stuart SBS40 shaking water bath was employed to heat the silver nanoparticle solutions. A sodium lamp (NAV-T 70 model from Osram China Lighting Co., Ltd.) was used as the light source for the photoinduced process.

**2.3. Shape Conversion of Silver Nanoplates under Heating and Photoinducing Conditions.** The initial triangular silver nanoplates were synthesized according to the Mirkin's method.<sup>49</sup> Briefly, an aqueous solution of AgNO<sub>3</sub> (0.1 mM, 100 mL), trisodium citrate (100 mM, 1.8 mL), PVP (0.06 g), and hydrogen peroxide (30 wt %, 0.24 mL) was mixed and vigorously stirred under ambient condition. NaBH<sub>4</sub> solution (100 mM, 1.5 mL) was then rapidly injected into the mixtures. After about 30 min, blue silver nanoprism solution was obtained.

The as-synthesized silver nanoprism solution was placed in a water bath at 95 °C. The color of silver nanoparticle solution changed from blue to purple, red and then yellow during the heating process (vials a–f in Figure 1). The obtained yellow silver nanoparticle solution after heating was irradiated under a sodium lamp. The color of silver nanoparticle solution changed to green. Finally, the blue silver nanoparticle solution was obtained again through the photoinduction process (vials f–h in Figure 1).

## 3. RESULTS AND DISCUSSION

The initial blue silver nanoprisms turned purple, red and yellow gradually within 4 min during the heating process at 95 °C (vials a–f in Figure 1). Colors of silver nanoparticles are related to their LSPR properties. The extinction spectra of silver nanoparticles were monitored to observe the evolution of LSPR properties in the process of heating (Figure 2A). The LSPR spectrum of the initial blue silver nanoparticle solution displays three bands centered at 333, 440, and 616 nm, which are assigned to the out-of-plane quadrupole, in-plane quadrupole, and in-plane dipole plasmon resonance modes of triangular silver nanoplates, respectively (curve a in Figure 2A).<sup>17,18</sup> The

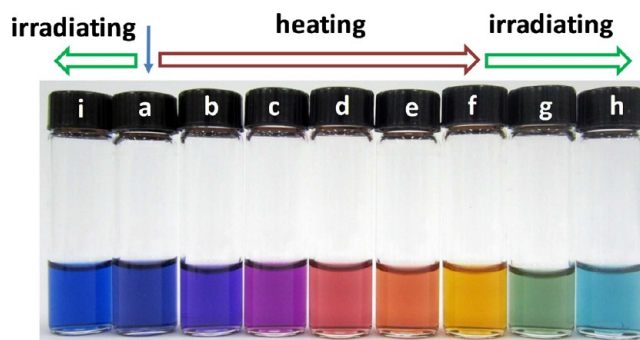


**Figure 1.** Photos of silver nanoparticle solutions during (a–f) heating and (f–h) subsequent light irradiation, and (i) after light irradiation prior to heating. Blue solid arrow denotes the initial silver nanoprism solution.

in-plane dipole plasmon resonance band of silver nanoprisms blue-shifted when the silver colloid was heated. This band changed to 462 nm when the silver nanoprisms were heated for 205 s (curve f in Figure 2A). Meanwhile, the out-of-plane quadrupole plasmon resonance band of silver nanoplates red-shifted to 340 nm from 333 nm, implying the aspect ratio (the ratio of length/diameter to thickness/height) of silver nanoplates decreased during heating process. These spectroscopic results indicate that heating caused morphological conversion of silver nanoparticles.

To gain insight into the evolution of silver nanoparticles, TEM was employed to observe shape transformation of silver nanoparticles at different heating times. Figure 3A–D show the TEM images of initial blue silver nanoparticles, and the silver nanoparticles with different colors obtained in the process of heating, respectively. As can be seen, all of the initial silver nanoparticles before heating are triangular nanoplates, with an edge length of  $28.2 \pm 3.3 \text{ nm}$  and a thickness of  $5.5 \pm 0.5 \text{ nm}$  (Figure 3A). The corner of triangular silver nanoplates became blunt after heating for 73 s (Figure 3B). The edge length and thickness of the truncated triangular silver nanoplates were measured to be  $25.0 \pm 2.7 \text{ nm}$  and  $5.9 \pm 0.6 \text{ nm}$ , respectively, from an edge-on view when the silver nanoplates stacked with each other and stood vertically on their edges on the TEM grids (Figure 3B). Silver nanoparticles with red color were obtained when the truncated triangular silver nanoplates were heated. TEM images reveal that most of the red silver nanoparticles are discal in shape, with a diameter of  $23.1 \pm 3.2 \text{ nm}$  and a thickness of  $7.1 \pm 0.6 \text{ nm}$  (Figure 3C). Finally, heating produced silver nanodisks with dimensions of  $19.6 \pm 3.2 \text{ nm}$  in diameter and  $7.2 \pm 0.4 \text{ nm}$  in thickness (Figure 3D). It has been suggested that increase in thickness of nanoplates could result in a drastic change in aspect ratio, which would cause a large shift in the LSPR band.<sup>46,49</sup> Detailed data on morphologies of silver nanoplates in different periods are shown in Table 1. The aspect ratio of silver nanoplates changed to 4.2 from 5.1 when silver nanoprisms were truncated by heating, and there was a small change in edge length (from  $28.2 \pm 3.3 \text{ nm}$  to  $25.0 \pm 2.7 \text{ nm}$ ). With regards to silver nanodisks (in red and yellow colors), the diameter of nanodisks decreased as the heating time increased. It is noted that the aspect ratios of silver nanoplates decreased in the process of heating, which is responsible for changes of LSPR of silver nanoplates involving blue-shift of in-plane dipole plasmon resonance band and red-shift of out-of-plane quadrupole plasmon resonance band.



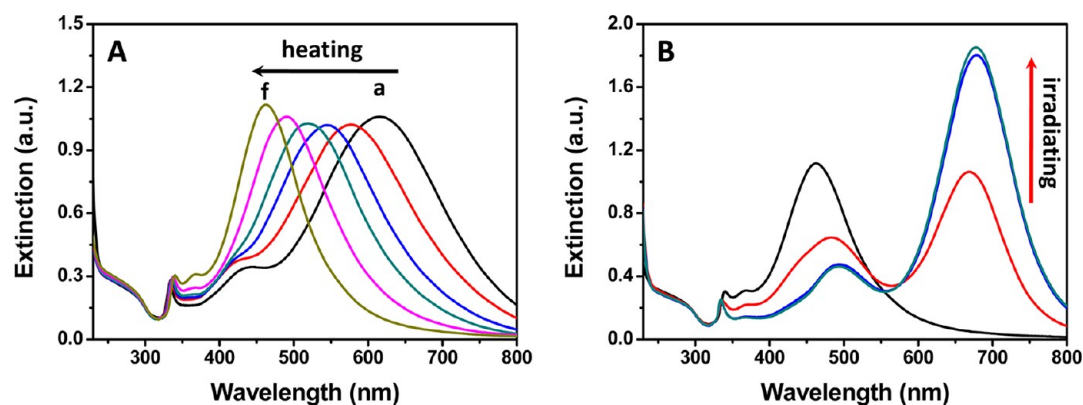


**Figure 2.** (A) Evolution of extinction spectra of silver nanoplates under heating for different time periods: (a) 0, (b) 30, (c) 73, (d) 125, (e) 169, and (f) 205 s. (B) Extinction spectra of heating-obtained silver nanoplates before and after light irradiation for 90, 210, and 270 min.

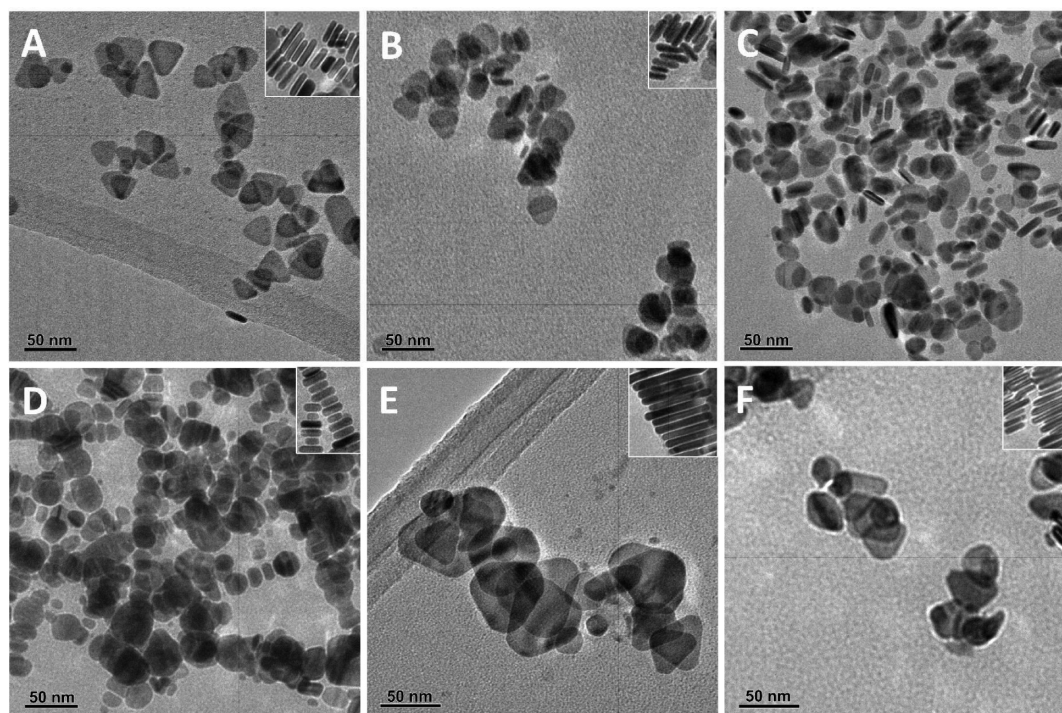


**Figure 3.** TEM images of (A) the initial silver nanoprisms, and the silver nanoplates obtained through heating for (B) 73, (C) 125, and (D) 205 s, (E) the silver nanoprisms transformed from silver nanodisks under light irradiation, and (F) the silver nanoplates from initial silver nanoprisms after light irradiation.

**Table 1. Data on Color, Shape, and Size of Silver Nanoplates in the Process of Shape Conversion under Heating and Irradiating**

| color          | shape                | length/diameter (nm) | thickness (nm) | aspect ratio |
|----------------|----------------------|----------------------|----------------|--------------|
| blue (initial) | triangular           | $28.2 \pm 3.3$       | $5.5 \pm 0.5$  | 5.1          |
| purple         | truncated triangular | $25.0 \pm 2.7$       | $5.9 \pm 0.6$  | 4.2          |
| red            | discal               | $23.1 \pm 3.2$       | $7.1 \pm 0.6$  | 3.3          |
| yellow         | discal               | $19.6 \pm 3.2$       | $7.2 \pm 0.4$  | 2.7          |
| blue (final)   | triangular           | $62.4 \pm 5.8$       | $9.2 \pm 0.4$  | 6.8          |

After heating treatment, the as-synthesized silver nanodisks with yellow color were irradiated under a sodium lamp. The silver nanodisk solution turned green from yellow, and finally blue under further irradiation (vials f–h in Figure 1). The

extinction spectra of silver nanoparticles during irradiation are depicted in Figure 2B. The LSPR band at 462 nm attributed to in-plane dipole plasmon resonance mode of silver nanodisks decreased during irradiation, which implies that the amount of silver nanodisks reduced in the reaction system. In the meantime, a new LSPR band centered around 670 nm appeared and increased in intensity during the irradiation process, which reveals that the silver nanoparticles with a new morphology were fabricated from nanodisks. The eventual extinction spectrum of silver nanoparticles after irradiation for 210 min displays three extinction peaks centered at 334, 493, and 678 nm. TEM characterization confirms that triangular silver nanoplates were prepared through conversion of silver nanodisks by photoinduction (Figure 3E). The edge length of triangular silver nanoplates transformed from nanodisks is  $62.4 \pm 5.8$  nm, and the thickness is  $9.2 \pm 0.4$  nm. The final triangular silver nanoplates from silver nanodisks are larger than

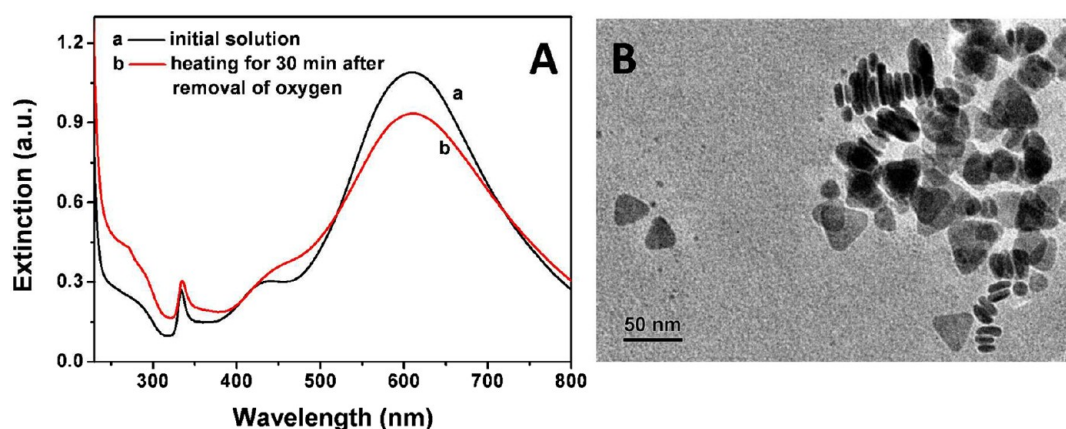


**Figure 4.** (A) Extinction spectra of (a) the initial silver nanoprism solution and (b) the silver nanoprism solution with removal of oxygen after heating for 30 min at 95 °C. (B) TEM image of the silver nanoprisms in the absence of oxygen after heating corresponding to curve b in (A).

the initial silver nanoprisms. The final silver nanoparticle solution from photoinduction was centrifuged. The bottom layer (precipitate), after redispersion in water, exhibits the spectral features of triangular silver nanoplates, with three LSPR bands at 334, 505, and 678 nm (curve b in Figure S1 in the Supporting Information).<sup>17,18</sup> The extinction spectrum of the supernatant after centrifugation shows extinction bands around 335, 480, and 660 nm, which are assigned to the small silver nanoplates unconverted to triangular silver nanoplates (curve c in Figure S1 in the Supporting Information). The TEM images of the bottom layer (precipitate) and upper layer (supernatant) of the final silver nanoparticle solution after centrifugation also testify the deduction from spectral results (see Figure S2 in the Supporting Information). The reconstruction of triangular silver nanoplates was realized from heating-obtained silver nanodisks through photoinduction process in the same reaction system. The as-synthesized triangular silver nanoplates changed slightly in LSPR spectrum after they were heated at 95 °C for 2 h (see Figure S3 in the Supporting Information), which indicates that the silver nanoplates obtained through photoinduction were stable even under prolonged heating.

In addition, light irradiation was performed on the initial silver nanoprisms to examine whether light can transform silver nanoprisms into nanodisks. The color of silver nanoparticle solution changed a bit after irradiation (vials a and i in Figure 1). The in-plane dipole plasmon resonance band at long wavelength of silver nanoprisms narrowed, increased in intensity and slightly red-shifted when the initial silver nanoprisms were irradiated (see Figure S4 in the Supporting Information), implying that the aspect ratio of silver nanoplates increased. TEM result demonstrates that the silver nanoplates after irradiation are still triangular, with an edge length of  $31.6 \pm 4.6$  nm and a thickness of  $6.5 \pm 0.4$  nm (Figure 2F), which suggests that irradiation changes the size but not the shape of initial silver nanoplates. Furthermore, the initial silver nanoprisms were heated at 95 °C and irradiated by sodium lamp simultaneously. The evolution of extinction spectra of silver nanoprism is depicted in Figure S5 in the Supporting Information. The main LSPR band at  $\sim 610$  nm blue-shifted to  $\sim 485$  nm that is assigned to in-plane dipole plasmon resonance mode of silver nanodisks, in 10 min. This indicates that the silver nanoprisms were transformed into silver nanodisks by heating even if the light irradiation was performed at the same time. The effect of light irradiation cannot block the shape conversion of silver nanoprisms through heating. The as-

synthesized silver nanodisks continued to be heated and irradiated simultaneously for 120 min. The final extinction spectrum shows complicated LSPR bands that are not the characteristic LSPR peaks of silver nanoprisms. Therefore, the spectral results imply that the silver nanodisks were not converted into silver nanoprisms under heating and irradiating together.

It is well-known that oxygen etching plays a critical role in synthesis of silver nanoparticles.<sup>50–52</sup> The oxygen was proved to etch the twinned silver particles to assist the fabrication of single crystal silver nanostructures via a polyol method.<sup>50–52</sup> In the present research, oxygen probably affects the shape conversion process from prism to disk under heating. To test this hypothesis, the initial silver nanoprism solution was bubbled by nitrogen gas and heated at 50 °C for 60 min simultaneously before heating performance at 95 °C. The initial silver nanoprism solution in sealed vial after removal of oxygen was heated for 30 min in water bath at 95 °C. Totally different from the case in which the dissolved oxygen in the silver colloid was not removed before heating, the initial silver nanoprism solution after removal of oxygen did not change much in color. The extinction spectrum of silver colloid with removal of oxygen after heating for 30 min is shown in Figure 4A. As can be seen, though there is some difference between the extinction spectra of silver nanoprism solutions before and after heating, the extinction spectrum of silver nanoparticle solution after heating displays the characteristic LSPR bands.<sup>17,18</sup> Furthermore, the TEM images show that the silver nanoparticles after heating are still triangular nanoplates (Figure 4B). These indicate that the initial silver nanoprisms could not be converted into silver nanodisks under heating in the absence of oxygen even when the heating time was extended to 30 min. The results demonstrate that the oxygen in solution assists the shape conversion from prism to disk in heating conditions because of its etching role.<sup>50–52</sup>

This shape conversion from nanoprism to nanodisk under heating seems to be similar to that in our previous research.<sup>30</sup> However, the shape conversion in the present study can be performed even if the concentration of citrate was 3.8 mM, much higher than that in previous report (0.2 mM). The citrate with higher concentration in this study did not block conversion from silver nanoprism to silver nanodisk under heating. Surface properties of silver nanoprisms prepared at room temperature here are markedly different from that prepared from the photoinduction method in previous



research.<sup>30</sup> The initial silver nanoprism solution was centrifuged to separate silver nanoprisms from original aqueous solution. Interestingly, the color of the silver nanoplates changed to purple, red, and yellow from blue gradually after deionized water was added into the precipitate of silver nanoprisms (upper panel in Figure 5), which is similar to the conversion

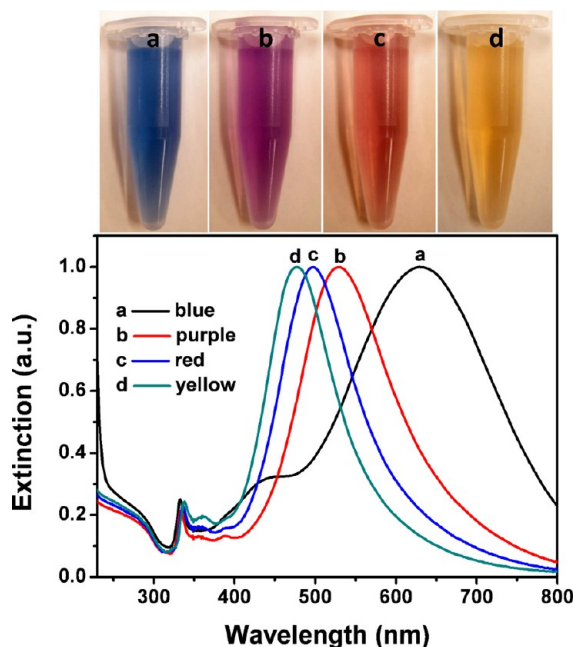


**Figure 5.** Upper panel: photos of (a) the initial silver nanoprism solution and (b–d) the precipitate of silver nanoprisms redispersed in deionized water for different times. Bottom panel: extinction spectra corresponding to silver nanoplate solutions in upper panel.

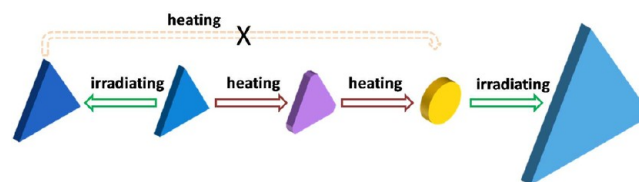
process of silver nanoplates under heating. The bottom panel in Figure 5 displays the corresponding extinction spectra of silver nanoparticles with different colors after deionized water was added. The changes of extinction spectra of silver nanoplates reveal that deionized water induced shape conversion from nanoprism to nanodisk. In addition to the extinction spectra, the TEM characterization demonstrate that the silver nanoprisms were converted to silver nanodisks after the precipitate of silver nanoprisms was redispersed in deionized water (see Figure S6 in the Supporting Information). Compared with solvent of the initial silver nanoprisms, the deionized water as fresh water has higher concentration of dissolved oxygen.<sup>53</sup> It is suggested that the more dissolved oxygen in deionized water boosts the shape conversion of the initial silver nanoprisms at room temperature. To further clarify the role of oxygen in deionized water induced shape conversion, we removed the dissolved oxygen in deionized water by bubbling with nitrogen gas and heating at 50 °C for 60 min simultaneously. The precipitate of silver nanoprisms was redispersed in the deionized water after removal of oxygen. The color of redispersed silver nanoprisms did not change observably. The extinction spectrum of silver nanoprisms redispersed in the deionized water after removal of dissolved oxygen still has the typical LSPR bands of silver nanoprisms when placed at room temperature for 24 h (see Figure S7A in the Supporting Information), which implies that the deionized water in the absence of oxygen was not able to transform silver nanoprisms into silver nanodisks. Besides, the TEM images show that the

silver nanoprisms did not change obviously in morphology when they were redispersed in deionized water after removal of oxygen (see Figure S7B in the Supporting Information). These results further prove that the oxygen in solution is pivotal in shape conversion from silver nanoprism to silver nanodisk. It should be noted that the as-synthesized initial silver nanoparticles did not change before they were centrifuged even though they were dispersed in water, which is probably due to lower concentration of oxygen in the initial solution than deionized water. It is proposed that heating can provide the initial solution with more energy to promote the role of oxygen in shape conversion of silver nanoprisms. Additionally, the precipitate of silver nanoprisms was redispersed in citrate aqueous solution ( $1 \times 10^{-3}$  M) to clarify the stabilizing role of citrate. It was found that the color of solution changed, which is similar to the case of deionized water (see Figure S8 in the Supporting Information). The results further demonstrate that the presence of citrate cannot prevent oxygen from changing the shape of silver nanoprisms.

Nevertheless, the color of silver nanoplates did not change obviously when ethanol was added in the precipitate of silver nanoprisms instead of deionized water. The extinction spectrum of silver nanoprisms redispersed in ethanol is similar to that of initial silver nanoprisms, besides slight red-shift of LSPR at long wavelength (see Figure S9A in the Supporting Information). This implies that the silver nanoplates did not change in shape when redispersed in ethanol, which is also demonstrated by TEM characterization (see Figure S9B in the Supporting Information). The silver nanoprisms redispersed in ethanol (in a sealed vial) were heated for 100 min at 95 °C. The color and extinction spectrum of silver nanoprisms in ethanol did not change obviously after heating (see Figure S10 in the Supporting Information), which indicates that the silver nanoprisms in ethanol are stable even at high temperature (95 °C). This is different from the case of silver nanoplates in deionized water. Though the concentration of dissolved oxygen in ethanol is higher than that in deionized water,<sup>54</sup> ethanol cannot convert the silver nanoprisms to nanodisks even at high temperature for a long time. It is inferred that the shape conversion of silver nanoprisms is influenced markedly by property of solvent besides oxygen in solution.

The conversion process of silver nanoplates under heating and light irradiation is illustrated in Scheme 1. The initial

#### Scheme 1. Illustration of the Shape Conversion of Silver Nanoplates under Heating and Light Irradiation



triangular silver nanoplates were truncated by heating with assistance of oxygen, and then converted into silver nanodisks. The diameter of silver nanodisks (19.6 nm) in yellow color solution is more than the diameter of inscribed circle of the initial nanoprism (16.3 nm), suggesting that the silver nanodisks were obtained through not only dissolving of silver atoms on the corner of silver nanoprisms but also readsorption of silver atoms on the side of nanoplates. Silver nanoprisms have been converted into silver nanodisks under heating in the

presence of a stabilizer (citrate) at a low concentration.<sup>30</sup> The shape conversion was realized through the migration of silver atoms from unstable sites to the stable ones, which was caused by the difference in surface energy and the selective adsorption of citrate. Moreover, the thickness of silver nanoplates did not change during shape conversion and the shape conversion just took place on basic planes of silver nanoplates. Yin et al. reported that the triangular silver nanoplates were converted into silver nanodisks by UV irradiation.<sup>37</sup> In their work, the thickness of silver nanoplates increased during transformation from triangular nanoplates to discal ones after irradiation of UV light. They suggested that the shape transformation involved a migration process of surface atoms of silver nanoplates. In the present study, the thickness of silver nanoplates increased by 1.7 nm (from 5.5 to 7.2 nm) during shape conversion from prism to disk through heating, which reveals that silver nanoplates changed in both direction of basic plane and height direction under heating. According to the Gibbs–Thomson effect, the sharp corners of silver nanoprisms have higher surface energy and are less stable, which could result in conversion from prism to disk by heat or light.<sup>21,30,46,55</sup> It is proposed that the shape conversion of silver nanoplates was completed through dissolving of silver atoms on less stable sites including sharp vertexes with high surface energy and readsorption of silver atoms to more stable sites with low surface energy.<sup>56,57</sup> The total volume of the nanoplates increased when the silver nanoprisms were converted into silver nanodisks with red color. It is possible that small silver nanoparticles in solution were involved in the rearrangement to silver nanodisk through the Ostwald ripening process driven by heating during conversion from nanoprism to nanodisk. The diameter of silver nanodisks decreased when the silver nanodisks in red solution were transformed into silver nanoprisms with yellow color during heating, but their thickness remained almost unchanged ( $7.1 \pm 0.6$  nm and  $7.2 \pm 0.4$  nm). It is suggested that only dissolving process of silver atoms on the sides of silver nanoplates happened during shrinking of silver nanodisks through heating. As can be found, many factors influence the process of shape conversion, such as the role of dissolved oxygen in solution, difference in surface energy corresponding to different parts of silver nanoparticles, and reaction temperature. The dissolved oxygen in solution possibly etched the parts with higher surface energy in the silver nanoprisms to assist the shape conversion from prism to disk. The selective oxidative etching during the shape conversion in the present research is different from the case of the previous report in which the interconversion between silver oxide particles and silver nanoparticles took place at room temperature.<sup>58</sup>

The silver nanodisks obtained by heating were transformed into silver nanoprisms under irradiation of light. This photoinduced shape conversion of silver nanoplates occurred in the same original silver nanoparticle solution. It has been suggested that the dipole plasmon excitation by light irradiation induces charge separation on the nanodisk surface and assists citrate photo-oxidation on the nanodisk surface.<sup>59,60</sup> The silver ions in solution were reduced by the citrate left in solution to become silver atoms that could contribute to growth and shape conversion of nanodisks. The small silver nanoparticles almost disappeared after photoinduction and the final nanoprisms were enlarged because of adsorption of silver atoms produced from photoinduced reduction by citrate. More citrate is not needed

to realize the photoinduced reaction, which is different from our previous study.<sup>48</sup>

PVP has been widely used to improve the stability of silver nanoparticles, assisting the synthesis of silver nanoplates.<sup>19,46,61–63</sup> The initial triangular silver nanoplates can be synthesized without PVP in a short time (less than 10 min), which was reported by Yin et al.<sup>64</sup> In this research, the silver nanoprisms without PVP were treated by heating as well. The evolution of extinction spectra was similar to those without PVP (see Figure S11A in the Supporting Information), which indicates that the silver nanoprisms without PVP were also transformed into silver nanodisks by heating. The heating-obtained silver nanodisks without PVP were irradiated by light. The changes of extinction spectra imply that the silver nanodisks without PVP were converted into silver nanoprisms through a photoinduced process (see Figure S11B in the Supporting Information). These results demonstrated that PVP does not influence the shape conversion of silver nanoplates under heating or light irradiation.

The color of silver nanodisks induced by deionized water did not change distinctly when the solution was irradiated under a sodium lamp. The extinction spectrum of silver nanoplates broadened a little and slightly blue-shifted after silver nanodisks were irradiated for more than 12 h without addition of citrate (curve b in Figure 6), indicating that the silver nanodisks were

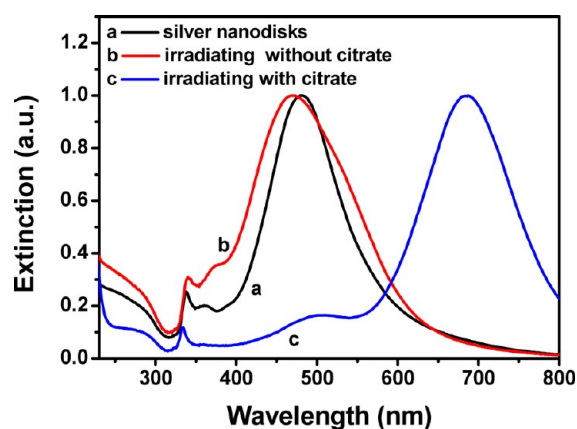


**Figure 6.** Extinction spectra of (a) the original silver nanodisks obtained through addition of deionized water in precipitate of silver nanoprisms, (b) the silver nanoplates after light irradiation for 12 h without addition of citrate, and (c) the silver nanoplates irradiated for 7 h after addition of citrate.

not converted into silver nanoprisms due to lack of citrate in the reaction solution after centrifugation. More citrate was added in the deionized water induced silver nanodisk solution to examine the role of citrate on the photoinduced shape conversion of silver nanoplates. The extinction spectrum of silver nanoplates displayed the characteristic LSPR bands of silver nanoprisms after light irradiation for 7 h in the presence of citrate (curve c in Figure 6). Tartrate containing dicarboxylate can be used to prepare silver nanoplates instead of citrate by Mirkin's method.<sup>49,64</sup> However, the extinction spectrum of deionized water induced silver nanodisks did not change visibly with 10 h irradiation (see Figure S12 in the Supporting Information) after addition of tartrate, revealing that the silver nanodisks cannot be transformed into triangular silver nanoplates by using tartrate instead of citrate under irradiation. These results demonstrate that citrate is essential

for the transformation from silver nanodisks to silver nanoprisms in photoinduced reaction.

#### 4. CONCLUSIONS

Shape conversion and reconstruction of triangular silver nanoplate were accomplished by heating and subsequent light irradiation in one reaction system. The initial silver nanoprisms were transformed to silver nanodisks by heating, and the LSPR property of silver nanoplate can be effectively adjusted by controlling the heating time. Oxygen in solution is proved to play a crucial role in shape conversion of silver nanoparticles from nanoprism to nanodisk. Moreover, the difference in surface energy of different parts of nanoplates is also a key factor causing the conversion from nanoprism to nanodisk. The silver nanodisks obtained from heating were reversed to silver nanoprisms just through light irradiation. Citrate is essential to the photoinduced conversion from silver nanodisks to silver nanoprisms. It is proposed that the citrate left in solution has a reduction effect on the surface of silver nanodisks under photoinduction, leading to reverse shape conversion of silver nanoplates. Shape conversion of silver nanoplates in the same system will allow effective tuning of optical properties of noble metal nanostructures.

#### ■ ASSOCIATED CONTENT

##### Supporting Information

Additional extinction spectra and TEM images of silver nanoparticles, as well as additional photograph of the solutions. This material is available free of charge via the Internet at <http://pubs.acs.org>.

#### ■ AUTHOR INFORMATION

##### Corresponding Author

\*E-mail: [xungai.wang@deakin.edu.au](mailto:xungai.wang@deakin.edu.au) (X.W.); [lu.sun@deakin.edu.au](mailto:lu.sun@deakin.edu.au) (L.S.).

##### Notes

The authors declare no competing financial interest.

#### ■ ACKNOWLEDGMENTS

This research was supported by the Central Research Grants Scheme and Alfred Deakin Postdoctoral Research Fellowship scheme at Deakin University, and partly by the National Natural Science Foundation of China (NSFC 20903043, 51273153).

#### ■ REFERENCES

- (1) Aslan, K.; Wu, M.; Lakowicz, J. R.; Geddes, C. D. *J. Am. Chem. Soc.* **2007**, *129*, 1524–1525.
- (2) Kleinman, S. L.; Ringe, E.; Valley, N.; Wustholz, K. L.; Phillips, E.; Scheidt, K. A.; Schatz, G. C.; Van Duyne, R. P. *J. Am. Chem. Soc.* **2011**, *133*, 4115–4122.
- (3) Lu, L.; Kobayashi, A.; Tawa, K.; Ozaki, Y. *Chem. Mater.* **2006**, *18*, 4894–4901.
- (4) Willets, K. A.; Van Duyne, R. P. *Annu. Rev. Phys. Chem.* **2007**, *58*, 267–297.
- (5) Sepúlveda, B.; Angelomé, P. C.; Lechuga, L. M.; Liz-Marzán, L. M. *Nano Today* **2009**, *4*, 244–251.
- (6) Arvizo, R. R.; Bhattacharyya, S.; Kudgus, R. A.; Giri, K.; Bhattacharya, R.; Mukherjee, P. *Chem. Soc. Rev.* **2012**, *41*, 2943–2970.
- (7) Huang, X.; Jain, P. K.; El-Sayed, I. H.; El-Sayed, M. A. *Nanomedicine* **2007**, *2*, 681–693.
- (8) Murphy, C. J.; Sau, T. K.; Gole, A. M.; Orendorff, C. J.; Gao, J.; Gou, L.; Hunyadi, S. E.; Li, T. *J. Phys. Chem. B* **2005**, *109*, 13857–13870.

- (9) Wiley, B. J.; Im, S. H.; Li, Z.-Y.; McLellan, J.; Siekkinen, A.; Xia, Y. *J. Phys. Chem. B* **2006**, *110*, 15666–15675.
- (10) Kelly, K. L.; Coronado, E.; Zhao, L. L.; Schatz, G. C. *J. Phys. Chem. B* **2003**, *107*, 668–677.
- (11) Gao, C.; Lu, Z.; Liu, Y.; Zhang, Q.; Chi, M.; Cheng, Q.; Yin, Y. *Angew. Chem., Int. Ed.* **2012**, *51*, 5629–5633.
- (12) Sherry, L. J.; Jin, R. C.; Mirkin, C. A.; Schatz, G. C.; Van Duyne, R. P. *Nano Lett.* **2006**, *6*, 2060–2065.
- (13) Haynes, C. L.; Van Duyne, R. P. *J. Phys. Chem. B* **2001**, *105*, 5599–5611.
- (14) Link, S.; Wang, Z. L.; El-Sayed, M. A. *J. Phys. Chem. B* **1999**, *103*, 3529–3533.
- (15) Jiang, X. C.; Yu, A. B. *Langmuir* **2008**, *24*, 4300–4309.
- (16) Hu, M.; Chen, J.; Marquez, M.; Xia, Y.; Hartland, G. *J. Phys. Chem. C* **2007**, *111*, 12558–12565.
- (17) Jin, R. C.; Cao, Y. W.; Mirkin, C. A.; Kelly, K. L.; Schatz, G. C.; Zheng, J. G. *Science* **2001**, *294*, 1901–1903.
- (18) Jin, R. C.; Cao, Y. C.; Hao, E.; Metraux, G. S.; Schatz, G. C.; Mirkin, C. A. *Nature* **2003**, *425*, 487–490.
- (19) Sun, Y. G.; Mayers, B.; Xia, Y. N. *Nano Lett.* **2003**, *3*, 675–679.
- (20) Hao, E.; Kelly, K. L.; Hupp, J. T.; Schatz, G. C. *J. Am. Chem. Soc.* **2002**, *124*, 15182–15183.
- (21) Chen, S.; Fan, Z.; Carroll, D. L. *J. Phys. Chem. B* **2002**, *106*, 10777–10781.
- (22) Wiley, B. J.; Xiong, Y.; Li, Z.-Y.; Yin, Y.; Xia, Y. *Nano Lett.* **2006**, *6*, 765–768.
- (23) Wiley, B. J.; Chen, Y.; McLellan, J. M.; Xiong, Y.; Li, Z.-Y.; Ginger, D.; Xia, Y. *Nano Lett.* **2007**, *7*, 1032–1036.
- (24) An, J.; Tang, B.; Zheng, X.; Zhou, J.; Dong, F.; Xu, S.; Wang, Y.; Zhao, B.; Xu, W. *J. Phys. Chem. C* **2008**, *112*, 15176–15182.
- (25) Lee, B.-H.; Hsu, M.-S.; Hsu, Y.-C.; Lo, C.-W.; Huang, C.-L. *J. Phys. Chem. C* **2010**, *114*, 6222–6227.
- (26) Tang, B.; Xu, S.; An, J.; Zhao, B.; Xu, W.; Lombardi, J. R. *Phys. Chem. Chem. Phys.* **2009**, *11*, 10286–10292.
- (27) Maillard, M.; Giorgio, S.; Pileni, M. P. *Adv. Mater.* **2002**, *14*, 1084–1086.
- (28) Jiang, L. P.; Xu, S.; Zhu, J. M.; Zhang, J. R.; Zhu, J. J.; Chen, H. Y. *Inorg. Chem.* **2004**, *43*, 5877–5883.
- (29) Xiong, Y.; Siekkinen, A. R.; Wang, J.; Yin, Y.; Kim, M. J.; Xia, Y. *J. Mater. Chem.* **2007**, *17*, 2600–2602.
- (30) Tang, B.; An, J.; Zheng, X.; Xu, S.; Li, D.; Zhou, J.; Zhao, B.; Xu, W. *J. Phys. Chem. C* **2008**, *112*, 18361–18367.
- (31) Chen, S. H.; Carroll, D. L. *Nano Lett.* **2002**, *2*, 1003–1007.
- (32) Chen, S.; Carroll, D. L. *J. Phys. Chem. B* **2004**, *108*, 5500–5506.
- (33) Sun, Y. G.; Wiederrecht, G. P. *Small* **2007**, *3*, 1964–1975.
- (34) Wang, R.; Liu, D.; Zuo, Z.; Yu, Q.; Feng, Z.; Liu, H.; Xu, X. *J. Mater. Chem.* **2012**, *22*, 2410–2418.
- (35) Zhang, J.; Langille, M. R.; Mirkin, C. A. *J. Am. Chem. Soc.* **2010**, *132*, 12502–12510.
- (36) Zhou, J.; An, J.; Tang, B.; Xu, S.; Cao, Y.; Zhao, B.; Xu, W.; Chang, J.; Lombardi, J. R. *Langmuir* **2008**, *24*, 10407–10413.
- (37) Pietrobon, B.; Kitaev, V. *Chem. Mater.* **2008**, *20*, 5186–5190.
- (38) Lu, H.; Zhang, H.; Yu, X.; Zeng, S.; Yong, K.-T.; Ho, H.-P. *Plasmonics* **2012**, *7*, 167–173.
- (39) Zheng, X.; Zhao, X.; Guo, D.; Tang, B.; Xu, S.; Zhao, B.; Xu, W.; Lombardi, J. R. *Langmuir* **2009**, *25*, 3802–3807.
- (40) Zhang, J.; Li, S.; Wu, J.; Schatz, G. C.; Mirkin, C. A. *Angew. Chem., Int. Ed.* **2009**, *48*, 7787–7791.
- (41) Bastys, V.; Pastoriza-Santos, I.; Rodriguez-Gonzalez, B.; Vainoras, R.; Liz-Marzán, L. M. *Adv. Funct. Mater.* **2006**, *16*, 766–773.
- (42) Zheng, X. L.; Xu, W. Q.; Corredor, C.; Xu, S. P.; An, J.; Zhao, B.; Lombardi, J. R. *J. Phys. Chem. C* **2007**, *111*, 14962–14967.
- (43) Pastoriza-Santos, I.; Liz-Marzán, L. M. *J. Mater. Chem.* **2008**, *18*, 1724–1737.
- (44) Rocha, T.; Winnischofer, H.; Westphal, E.; Zanchet, D. *J. Phys. Chem. C* **2007**, *111*, 2885–2891.
- (45) Stamplecoskie, K. G.; Scaiano, J. C. *J. Am. Chem. Soc.* **2010**, *132*, 1825–1827.



- (46) Zhang, Q.; Ge, J.; Pham, T.; Goebel, J.; Hu, Y.; Lu, Z.; Yin, Y. *Angew. Chem., Int. Ed.* **2009**, *48*, 3516–3519.
- (47) An, J.; Tang, B.; Ning, X.; Zhou, J.; Xu, S.; Zhao, B.; Xu, W.; Corredor, C.; Lombardi, J. R. *J. Phys. Chem. C* **2007**, *111*, 18055–18059.
- (48) Tang, B.; Xu, S.; An, J.; Zhao, B.; Xu, W. *J. Phys. Chem. C* **2009**, *113*, 7025–7030.
- (49) Metraux, G. S.; Mirkin, C. A. *Adv. Mater.* **2005**, *17*, 412–415.
- (50) Wiley, B.; Herricks, T.; Sun, Y.; Xia, Y. *Nano Lett.* **2004**, *4*, 1733–1739.
- (51) Zhang, H.; Jin, M.; Xia, Y. *Angew. Chem., Int. Ed.* **2012**, *51*, 7656–7673.
- (52) Liang, H.; Zhao, H.; Rossouw, D.; Wang, W.; Xu, H.; Botton, G. A.; Ma, D. *Chem. Mater.* **2012**, *24*, 2339–2346.
- (53) Benson, B. B.; Krause, D. *Limnol. Oceanogr.* **1984**, *29*, 620–632.
- (54) Shchukarev, S. A.; Tolmacheva, T. A. *J. Struct. Chem.* **1968**, *9*, 6–21.
- (55) Millstone, J. E.; Metraux, G. S.; Mirkin, C. A. *Adv. Funct. Mater.* **2006**, *16*, 1209–1214.
- (56) Zeng, Q.; Jiang, X.; Yu, A.; Lu, G. *Nanotechnology* **2007**, *18*, 035708.
- (57) Jiang, X.; Zeng, Q.; Yu, A. *Nanotechnology* **2006**, *17*, 4929–4935.
- (58) Gallardo, O. A. D.; Moiraghi, R.; Macchione, M. A.; Godoy, J. A.; Perez, M. A.; Coronado, E. A.; Macagno, V. A. *RSC Advances* **2012**, *2*, 2923–2929.
- (59) Xue, C.; Metraux, G. S.; Millstone, J. E.; Mirkin, C. A. *J. Am. Chem. Soc.* **2008**, *130*, 8337–8344.
- (60) Wu, X.; Redmond, P. L.; Liu, H.; Chen, Y.; Steigerwald, M.; Brus, L. *J. Am. Chem. Soc.* **2008**, *130*, 9500–9505.
- (61) Wiley, B. J.; Sun, Y.; Xia, Y. *Acc. Chem. Res.* **2007**, *40*, 1067–1076.
- (62) Zhang, J.; Liu, H.; Zhan, P.; Wang, Z.; Ming, N. *Adv. Funct. Mater.* **2007**, *17*, 1558–1566.
- (63) Deivaraj, T. C.; Lala, N. L.; Lee, J. Y. *J. Colloid Interface Sci.* **2005**, *289*, 402–409.
- (64) Zhang, Q.; Li, N.; Goebel, J.; Lu, Z.; Yin, Y. *J. Am. Chem. Soc.* **2011**, *133*, 18931–18939.